

Magnetic nanostructures on the fcc Fe/Cu(100) surface

V. S. Stepanyuk, W. Hergert, and P. Rennert

Fachbereich Physik, Martin-Luther-Universität, Fr.-Bach-Platz 6, D-06099 Halle, Germany

B. Nonas, R. Zeller, and P. H. Dederichs

Institut für Festkörperforschung, Forschungszentrum Jülich, D-52425 Jülich, Germany

(Received 26 January 1999)

We present systematic *ab initio* calculations for the magnetic moments of 3*d* and 4*d* transition-metal impurities on the high-moment ferromagnetic phase of fcc Fe/Cu(100) surface. We find that on this substrate the moments of the impurities are in general larger than on bcc Fe. Furthermore the transition from antiferromagnetic to ferromagnetic coupling occurs at smaller valencies. A very subtle behavior is found for Ru nanostructures, which show ferromagnetic coupling for adatoms and linear chains, but antiferromagnetic coupling for larger islands and monolayers.

I. INTRODUCTION

Epitaxial growth of thin films offer the unique opportunity to stabilize systems in metastable states. In that regard Fe films on Cu(100) attracted much attention, because the fcc phase of iron can be grown epitaxially at low temperatures.¹⁻⁴ In the bulk fcc Fe exists only at high temperatures. Fe grows on Cu(100) pseudomorphically because a small negative misfit of about 1% forces only a slightly increased lattice spacing of the Fe and a small tetragonal distortion. First principle calculations predicted that an increased lattice constant may stabilize a ferromagnetic (FM) ground state in the otherwise antiferromagnetic (AF) fcc Fe.⁵ Due to a small misfit for the AF fcc Fe phase ($a=3.58$ Å) and the FM fcc Fe phase ($a=3.66$ Å), a small lattice distortion can drive Fe/Cu(100) into either AF or FM states, thus leading to a magnetic instability. In Fe films grown on Cu(100) one distinguishes a high-moment FM, a low-moment FM and low-moment AF phases.⁵ Experimentally, both ferromagnetism and antiferromagnetism have been observed.⁶⁻¹¹ FM fcc Fe can be grown up to 4–5 monolayers (ML). For larger coverages (up to 11 ML), fcc Fe films prefer antiferromagnetic or noncollinear configurations. The transformation into FM bcc Fe takes place for coverage more than 11 ML.

One of the important problems in the interface magnetism is the coupling of magnetic materials across an interface. The contact of magnetic and nonmagnetic materials with magnetic substrates can show many interesting properties, which are strongly determined by the hybridization between the electronic states at interfaces. There are especially theoretical and experimental activities on magnetic properties of 3*d* systems on the bcc Fe(100) substrate.¹²⁻¹⁴ The transition from antiferromagnetic to ferromagnetic coupling in the middle of the *d* series has been recently predicted in *ab initio* calculations for 3*d* adatoms¹² and 3*d* monolayers on Fe(100) surface.¹³ Experimental investigations of 3*d* layers on the Fe(001) surface demonstrated a complicated and contradictory picture of the magnetic coupling and indicated that the structure of the surfaces and interfaces plays an important role in forming of magnetic states.¹⁴

Growing of nonmagnetic in bulk 4*d* metals on metallic surfaces may add another possibility for obtaining magnetic nanostructures. Unusual magnetic properties of 4*d* elements have been predicted for monolayers, free and supported clusters.¹⁵ Evidence of 4*d* magnetism has been found in experiments with free clusters, adatoms and supported clusters on noble metal substrates and Ru monolayers on C(0001).¹⁶ Recent experimental studies of Rh/Fe(100),¹⁷ Ru/Fe(100),¹⁸ and Pd/Fe(100)¹⁹ multilayers demonstrated that 4*d* materials exhibit induced magnetic moments. The largest magnetic moment ($1\mu_B$) was found for Rh. The deposition of magnetic and nonmagnetic elements on fcc Fe/Cu(100) may provide a new class of magnetic materials. The main goal of our paper is to show that many interesting and unusual magnetic properties exist in nanostructures on fcc Fe/Cu(100) surface. In this paper we concentrate on the high moment ($M=2.76\mu_B$) ferromagnetic phase of fcc Fe/Cu(100). A monolayer thick Fe film on Cu(100) is considered. We demonstrate that many 3*d* and 4*d* atoms exhibit a large magnetic moments on the fcc Fe/Cu(100) and compare the results with calculations for the bcc Fe(100) substrate.¹² We find that on the fcc Fe/Cu(100) substrate the moments of the impurities are in general larger than on the bcc Fe. Furthermore the transition from antiferromagnetic to ferromagnetic coupling occurs at smaller valencies. A very subtle behavior is found for Ru nanostructures, which show ferromagnetic coupling for adatoms and linear chains, but antiferromagnetic coupling for larger islands and monolayers.

II. COMPUTATIONAL ASPECTS

The first principle calculations performed in this paper are based on the local approximation of density functional theory and on the KKR Green's function method for low-dimensional systems developed in our group.²⁰ We treat a surface as a two-dimensional perturbation of the bulk. Taking into account the 2D periodicity of the ideal surface, one can find the structural Green's function, by solving a Dyson equation. This Green's function is then used as the reference Green's function to calculate the Green's function of the perturbed system with adatoms and clusters on the surface. By

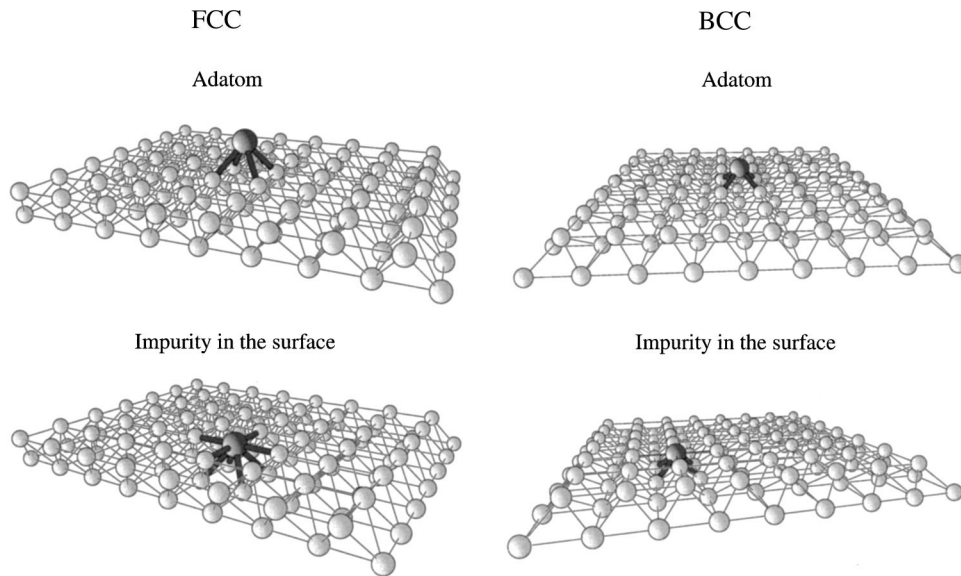


FIG. 1. Geometrical arrangement of adatoms (H) and impurities (T) on the fcc Fe/Cu(100) and the bcc Fe(100) surfaces. Bonds of adatoms and impurities to the first nearest neighbors are shown.

multipole expansion up to $l_{\max}=6$ we take the full charge density into account. Coulomb and exchange-correlation energies are calculated using $l_{\max}=12$. We allow the potentials of all adatoms and of all reference sites adjacent to the adatoms to be perturbed. Details concerning the calculations can be found in previous works.²⁰ Calculations are performed for adatoms, supported clusters and impurities in the surface layer. Relaxations are not included in the present calculations. The adatoms, impurities and the atoms of clusters studied here occupy ideal lattice sites: hollow (H) or terrace (T) sites. The nearest neighbor distance of atoms in clusters is the nearest-neighbor distance of the Cu lattice. Geometrical arrangement of adatoms and impurities on fcc Fe/Cu(100) and bcc Fe(100) is shown in Fig. 1. The magnetic moments of 3d and 4d adatoms on fcc Fe/Cu(100) are calculated by ignoring changes in the distances between adatoms and the surface caused by relaxation. The adatom-surface distance on Fe(100) is about 2.8% shorter than the one for fcc Fe/Cu(100) (see Fig. 1). Nevertheless, we will demonstrate that magnetic moments of 3d adatoms are very close on both substrates. Also, it will be shown that general trends in magnetic coupling of 4d adatoms with Fe on fcc Fe/Cu(100) and Fe(100) are the same. Due to simple size arguments for 4d impurities on fcc Fe/Cu(100) surface we expect outward relaxations and slight enhancement of the magnetic moments as compared to the below results. In most cases the relaxation energies are small compared to the corresponding spin polarization energies. For example, for 3d impurities in Fe bulk¹² and for 3d monolayers on the Fe(100) (Ref. 13) relaxations energies are less than 0.02 eV. No switch from one magnetic coupling to any other one was found during the interlayer relaxation for 3d monolayers on the Fe(100).¹³ Therefore, we do not expect that lattice relaxations can seriously affect the calculated moments.

III. RESULTS AND DISCUSSION

A. 3d atoms in H and T sites

First, we discuss magnetic moments obtained for 3d atoms in H sites on the fcc Fe/Cu(100) surface and compare

the results with calculations for Fe(100).¹² We find [see Fig. 2(a)] that all 3d adatoms on the fcc Fe/Cu(100) surface are magnetic. In Fig. 2 a positive moment means ferromagnetic and negative one means antiferromagnetic coupling with Fe. Among the 3d adatoms the largest local moments are obtained for Cr (AF) and Mn (F). In the middle of the series the moment curve changes from negative to positive values, i.e., the adatoms on the left side of the series couple antiferromagnetically with the Fe monolayer, while the adatoms on the right side couple ferromagnetically to the Fe. In this sense, the present results are very similar to results obtained for adatoms and monolayers on Fe(100) surface.^{12,13} Large magnetic moments for all adatoms on fcc Fe/Cu(100), except Ni and Sc are determined by reduced dimensionality, rather

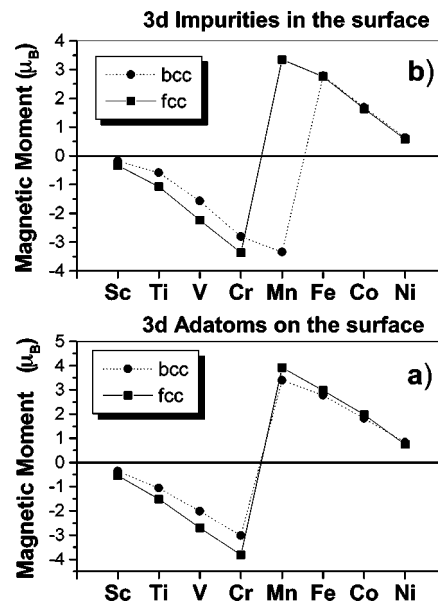


FIG. 2. (a) Magnetic moments of 3d atoms in hollow (H) positions on fcc Fe/Cu(100) and Fe(100) surfaces. (b) Magnetic moments of 3d atoms in terrace (T) positions of fcc Fe/Cu(100) and Fe(100) surfaces.

by the hybridization between adatoms and the magnetic substrate. It becomes clear, if one compares moments for 3d adatoms on fcc Fe/Cu(100) and Cu(100) surfaces.²⁰ Indeed, in all cases, except Ni and Sc, the hybridization between the *d*-states of the adatoms and the Fe substrate reduces moments. The Ni and Sc adatoms are non magnetic on Cu(100) surface,²⁰ but they have magnetic moments on fcc Fe/Cu(100) substrate. Thus, the moments of Ni and Sc are induced by the hybridization of their electronic states with electronic states of the Fe atoms, while the hybridization reduces the moments of all other 3d adatoms.

Comparing moments of the 3d adatoms on fcc Fe/Cu(100) and bcc Fe(100) surfaces, one should note that the distance between adatoms and the first nearest neighbors on the bcc substrate ($d_{\text{bcc}}=2.48$ Å) is smaller than on the fcc one ($d_{\text{fcc}}=2.55$ Å) (see Fig. 1), which increases the *d-d* hybridization with the Fe atoms on Fe(100). It is seen [see Fig. 2(a)] that, except Ni, the moments of 3d adatoms are slightly reduced on Fe(100). A small enhancement of the moment of the Ni adatom on Fe(100) compared to fcc Fe/Cu(100) can be understood recalling our former investigations on impurities, adatoms, and supported clusters.^{20,21} We showed that due to the *d-d* interactions, the *d* states of impurities, adatoms, and monolayers at the end of the *d* series are shifted to higher energies, leading to an increase of the LDOS at Fermi energy and thus to higher moments. The moment of the Ni atom is larger on Fe(100) due to increased hybridization with Fe atoms.

A comparison of the magnetic moments of 3d atoms in *T* sites of fcc Fe/Cu(100) and Fe(100) is presented in Fig. 2(b). In the *T* sites there are 4 nearest neighbors in bcc and 8 in fcc (see Fig. 1). Thus, the increasing coordination number in fcc Fe/Cu(100) tends to decrease the moments compared to Fe(100). From the other side, the larger interatomic distances in fcc Fe/Cu(100) tend to decrease the hybridization of impurities orbitals with 3d orbitals of Fe. According to the investigations of Liu *et al.*²² the effect of interatomic distances on the magnetic moments is larger than the coordination number. Our results show [see Fig. 2(b)] that for early 3d impurities this is indeed true: the moments of Sc, Ti, V, and Cr on fcc Fe/Cu(100) are larger (but negative) than the ones on Fe(100). The more or less equal moments obtained for Fe, Co, and Ni are basically a consequence of the fact that in all these cases the majority states are practically filled, so that the moments are more or less saturated.

A most interesting case is Mn. The local moment of the Mn adatom couples ferromagnetically to fcc Fe/Cu(100) and to Fe(100) substrates, while for the Mn surface atom in Fe(100) the antiferromagnetic configuration is most stable, lying 0.34 eV lower than the ferromagnetic one. The ground state of the Mn impurity in fcc Fe/Cu(100) is ferromagnetic and lies 0.034 eV below the antiferromagnetic solution. Thus, both solutions are nearly degenerate. A complicated and curious magnetic behavior was also found in experiments on Mn/Fe interfaces.²³ For example, experiments by means of spin-polarized electron-energy loss spectroscopy detected antiparallel coupling between 1 ML of Mn and Fe on Fe(100), but for low coverage a parallel coupling was found.²⁴ The study of Mn films on Fe(100) by soft x-ray magnetic circular dichroism showed that up to 2 ML the Mn/Fe interfacial coupling is ferromagnetic. Magnetic circu-

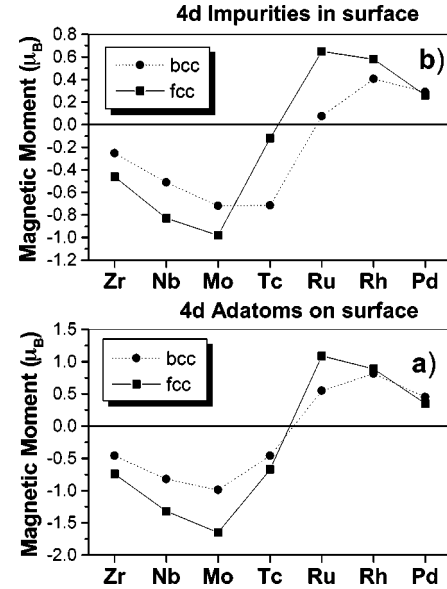


FIG. 3. (a) Magnetic moments of 4d atoms in hollow (*H*) positions on fcc Fe/Cu(100) and Fe(100) surfaces. (b) Magnetic moments of 4d atoms in terrace (*T*) positions of fcc Fe/Cu(100) and Fe(100) surfaces.

lar dichroism experiments revealed that for a small level of ML coverage the magnetic moment of Mn is antiparallel to the Fe substrate.²⁵ Recent *ab initio* calculations for Mn monolayers on the Fe(100) predicted that the ferrimagnetic state is expected around one monolayer, but for a Mn thickness beyond one monolayer, ferromagnetic or layered antiferromagnetic Mn films should be more stable.¹³ It is also useful to recall our recent investigations on Mn clusters on Ag and Cu surfaces.²⁶ We have shown that supported Mn clusters exhibit magnetic bistability. Recently, Sessoli *et al.*²⁷ reported the observation of magnetic bistability of ligated Mn₁₂ metal ion clusters. Thus, the magnetic properties of Mn nanostructures depend critically on the structural and chemical environment.

B. 4d atoms in *H* and *T* sites

We now consider results for 4d atoms. Figure 3(a) shows a comparison of the local moments of the 4d atoms on fcc Fe/Cu(100) and Fe(100) in *H* sites. The general trend in magnetic coupling of 4d adatoms with Fe atoms is similar for both substrates: antiferromagnetic coupling to Fe is found for early 4d impurities and ferromagnetic for the late ones. All adsorbate atoms, except Pd, have larger magnetic moments on the fcc substrate than on the bcc one due to the reduced hybridization mentioned above. The Pd free atom is nonmagnetic. Also, the Pd atoms are nonmagnetic on the Cu surface.²⁰ Thus, a sizeable magnetic moments of the Pd atoms on both substrates are determined by the direct hybridization of 4d states of Pd with 3d states of Fe atoms. The results for both isoelectronic Pd and Ni are similar: moments on the bcc substrate are larger than ones on the fcc due to stronger hybridization with Fe atoms. Due to the larger extent of the 4d wave functions, the difference between moments on the bcc and fcc substrates is more pronounced for 4d atoms compared to 3d ones (see Fig. 2). The tendency for magnetism is reduced for 4d atoms.

Figure 3(b) shows the local moments of the $4d$ atoms in T positions of fcc Fe/Cu(100) and Fe(100) surfaces. Considering these results one should note, that the number of nearest neighbors on the bcc (100) surface does not change on going from hollow to the terrace position, but the number of next nearest neighbors changes from 1 to 5. Due to extended $4d$ wave functions, the moments of $4d$ atoms in T positions are influenced by the hybridization of $4d$ states with $3d$ states of the next nearest neighbors Fe atoms. On the fcc (100) surface the number of the first nearest neighbors changes from 4 to 8 going from the hollow site to the terrace position. The larger number of the nearest neighbors near the $4d$ impurity in fcc Fe/Cu(100) tends to decrease moments compared to Fe(100). On the other hand, the larger interatomic distances in fcc Fe/Cu(100) tend to increase the moments. Additionally, the magnetic behavior of $4d$ impurities in Fe(100) is strongly influenced by surface states of the bcc surface. For example, unusual enhancement of the moment of the Tc in the T position of Fe(100) was found in our former calculations.¹² Figure 3(b) shows that, except for Tc and Pd, the moments of all $4d$ impurities in fcc Fe/Cu(100) are enhanced compared to Fe(100).

IV. RU CLUSTERS AND MONOLAYERS

We perform calculations for Ru, Rh, and Pd monolayers on fcc Fe/Cu(100) surface. In Table I we present our results

TABLE I. Magnetic moment of $4d$ atoms in monolayers and bilayers deposited on fcc Fe/Cu(001) and Fe(001) substrates. (All moments are given in μ_B .)

System	Theory	Experiment
Pd/Fe/Cu(001)	0.23	
Pd/Fe(001)	0.29 (Ref. 17)	0.4 (Ref. 19)
Rh/Fe/Cu(001)	0.1	
Rh/Fe(001)	0.82 (Refs. 17,28)	> 1 (Ref. 18)
Ru/Fe/Cu(001)	-0.25	
Ru/Fe(001)	0.36 (Ref. 28), 0.49 (Ref. 17)	0.5 (Ref. 18)
Fe/Ru/Fe/Cu(001)	-0.26	
Fe/Ru/Fe(001)	0.36 (Ref. 28)	

for monolayers and results obtained for Fe(100) in experiments and in first principle calculations. Moments of Rh and Pd monolayers are reduced on the fcc surface compared to the bcc. The reduction of the moment is very strong for Rh. These results clearly show that the driving mechanism for the magnetism of the overlayers can be attributed to the hybridization between overlayers and the Fe substrate, which is stronger on the bcc surface. Ru atoms represent the most interesting case. Surprisingly, we found that Ru monolayers are antiferromagnetically coupled to the Fe on fcc Fe/Cu(100). This is in contrast with results obtained for Fe(100). An additional Fe monolayer does not change the

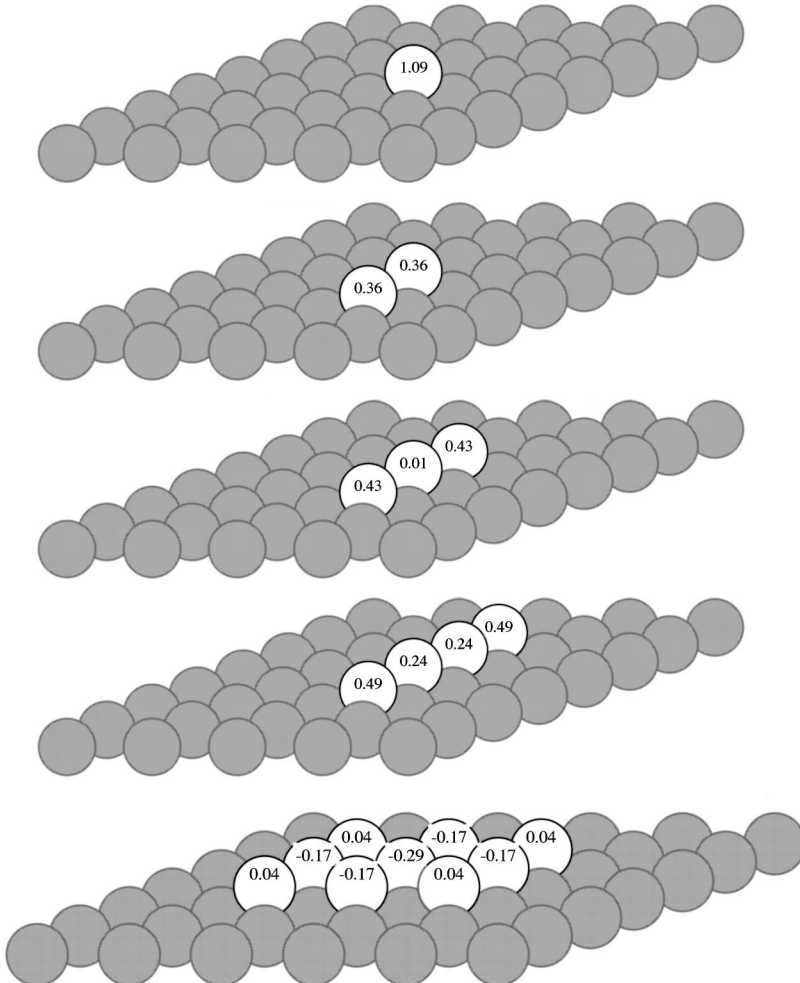


FIG. 4. Magnetic moment of Ru clusters on fcc Fe/Cu(100). The linear chains are orientated in the (110) direction. All moments are given in Bohr magnetons.

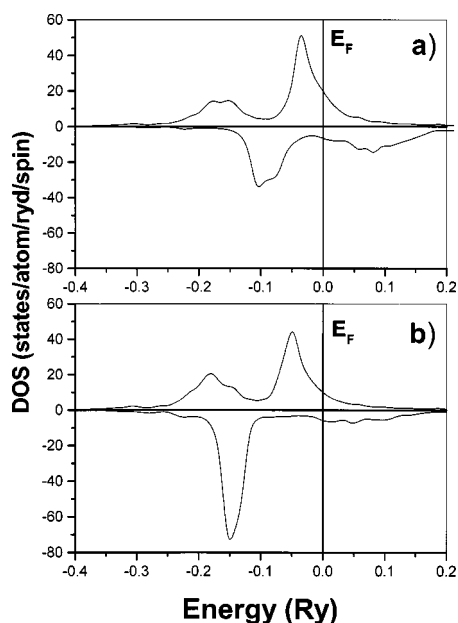


FIG. 5. LDOS (d component only) of Ru atoms. (a) The single Ru adatom on fcc Fe/Cu(100); (b) the Ru atom in the Ru_9 cluster on fcc Fe/Cu(100).

antiferromagnetic coupling of the Ru monolayer to the Fe. The Ru monolayers in the Fe/Ru/Fe/Cu(100) and Ru/Fe/Cu(100) sandwiches have very similar magnetic moments. It is an evidence that the overlayer-substrate hybridization is the main cause of the antiferromagnetic coupling between Ru and fcc Fe/Cu(100). In order to get a deeper insight into the unusual behavior of Ru atoms on fcc Fe/Cu(100) we perform calculations for a small Ru clusters. These calculations show an evolution in magnetism with cluster growth. Results for some selected clusters are presented in Fig. 4.²⁹ One can see that small linear chains of Ru are ferromagnetic and ferromagnetically coupled to the Fe. At the same time, in small plane islands of 9 atoms the transition from ferromagnetic to antiferromagnetic coupling is found. The central atom in the plane island of nine atoms has the same coordination as atoms in monolayers. One can see, that the moment

of this atom is very close to the moment of atoms in the Ru monolayer. Thus, the interaction between Ru atoms on fcc Fe/Cu(100) leads to the transition from ferromagnetic to antiferromagnetic coupling. To understand the nature of the results for the Ru, we perform calculations for LDOS of the Ru adatom on fcc Fe/Cu(100) and for the Ru atom in the cluster of nine atoms. In Fig. 5 LDOS for both cases are presented. The interaction between Ru atoms mainly influence the minority states and shifts these states to the lower energies. It leads to the ferromagnetic-antiferromagnetic transitions in Ru nanostructures.

V. CONCLUSIONS

In conclusion, we have performed extensive first principle calculations to determine magnetic moments of $3d$ and $4d$ impurities on the high-moment phase of fcc Fe/Cu(100) surface. Our results show that all $3d$ and $4d$ impurities in the terrace position and as adatoms are magnetic. Compared to results for Fe(100), moments of all atoms, except Ni, Tc, and Pd are enhanced on fcc Fe/Cu(100). The transition from antiferromagnetic to ferromagnetic coupling to the Fe atoms occur for the $3d$ atoms on both substrates between Cr and Mn and for the $4d$ ones between Tc and Ru. For the $3d$ impurities in the surface the behavior is more complicated, since due to the stronger hybridization the transition is shifted for the bcc Fe substrate to higher valencies. Small Ru clusters exhibit a very delicate balance between ferromagnetic and antiferromagnetic coupling. Whereas the Ru adatom and small chains of Ru atoms couple ferromagnetically to the fcc Fe substrate, a Ru monolayer and small square islands prefer an antiferromagnetic coupling. We hope that the present calculations will motivate experimental efforts to study magnetic nanostructures on the metastable fcc phase of Fe.

ACKNOWLEDGMENTS

We thank J. Kirschner and J. Shen for helpful discussions. Calculations were performed on a Cray computer of the German supercomputer center (HLRZ). This project was supported by Deutsche Forschungsgemeinschaft (DFG).

¹W.A. Jesser and J.W. Matthews, *Philos. Mag.* **15**, 1097 (1967); **17**, 595 (1968).

²D.P. Pappas, K.P. Kämper, and H. Hopster, *Phys. Rev. Lett.* **64**, 3175 (1990).

³J. Thomassen, F. May, B. Feldmann, M. Wuttig, and H. Ibach, *Phys. Rev. Lett.* **69**, 3831 (1992).

⁴J. Giergiel, J. Shen, J. Woltersdord, A. Kirilyuk, and J. Kirschner, *Phys. Rev. B* **52**, 8528 (1995).

⁵V.L. Moruzzi, P. Marcus, and J. Kübler, *Phys. Rev. B* **39**, 6957 (1989); T. Kraft, P.M. Marcus, and M. Scheffler, *ibid.* **49**, R11511 (1994).

⁶D. Li, M. Freitag, J. Pearson, Z.Q. Qiu, and S.D. Bader, *J. Appl. Phys.* **76**, 6425 (1994).

⁷Th. Detzel, M. Vonbank, M. Denath, and V. Dose, *J. Magn. Magn. Mater.* **147**, L1 (1995).

⁸W.A. Macedo and W. Keune, *Phys. Rev. Lett.* **61**, 475 (1988).

⁹C. Liu, E.R. Moog, and S.D. Bader, *Phys. Rev. Lett.* **60**, 2422 (1988).

¹⁰M. Wuttig and J. Thomassen, *Surf. Sci.* **282**, 237 (1993); S. Müller, P. Byer, C. Reische, K. Heinz, B. Feldmann, H. Zillger, and M. Wittig, *Phys. Rev. Lett.* **74**, 765 (1995).

¹¹T. Asada and S. Blügel, *Phys. Rev. Lett.* **79**, 507 (1997).

¹²B. Nonas, K. Wildberger, R. Zeller, and P.H. Dederichs, *J. Magn. Magn. Mater.* **165**, 137 (1997); B. Nonas, K. Wildberger, R. Zeller, P.H. Dederichs, and B.L. Gyorffy, *Phys. Rev. B* **57**, 84 (1998).

¹³S. Handschuh and S. Blügel, *Solid State Commun.* **105**, 633 (1998).

¹⁴G. Panaccione, F. Sirotti, E. Narducci, and G. Rossi, *Phys. Rev. B* **55**, 389 (1997).

¹⁵B.V. Reddy, S.N. Khanna, and B.L. Dunlap, *Phys. Rev. Lett.* **70**, 3323 (1993); M.J. Zhu, D.M. Bylander, and L. Kleinman, *Phys.*

- Rev. B **43**, 4007 (1991); K. Wildberger, V.S. Stepanyuk, P. Lang, R. Zeller, and P.H. Dederichs, Phys. Rev. Lett. **75**, 509 (1995).
- ¹⁶A.J. Cox, J.G. Louderback, and L.A. Bloomfield, Phys. Rev. Lett. **71**, 923 (1993); H. Beckmann and G. Bergmann, Phys. Rev. B **55**, 14 350 (1997); R. Pfandzelter, G. Stecerl, and C. Rau, Phys. Rev. Lett. **74**, 3467 (1995).
- ¹⁷T. Kachel, W. Gudat, C. Carbone, E. Vescovo, S. Blügel, U. Alkemper, and W. Eberhardt, Phys. Rev. B **46**, R12 888 (1992).
- ¹⁸K. Totland, P. Fuchs, J.C. Gröbli, and M. Landolt, Phys. Rev. Lett. **70**, 2487 (1993); T. Lin, M.A. Tomaz, M.M. Schwickert, and G.R. Harp, Phys. Rev. B **58**, 862 (1998); O. Rader, C. Carbone, W. Clemens, E. Vescovo, S. Blügel, and W. Eberhardt, *ibid.* **45**, 13 823 (1992).
- ¹⁹E.E. Fullerton, D. Stoeffler, K. Ounadjela, B. Heinrich, Z. Celen-ski, and J.A.C. Bland, Phys. Rev. B **51**, 6364 (1995); J. Vogel, A. Fontaine, V. Cros, F. Petroff, J.P. Kappler, G. Krill, A. Rogalev, and J. Goulon, *ibid.* **55**, 3663 (1997).
- ²⁰V.S. Stepanyuk, W. Hergert, K. Wildberger, R. Zeller, and P.H. Dederichs, Phys. Rev. B **53**, 2121 (1996); V.S. Stepanyuk, W. Hergert, P. Rennert, K. Wildberger, R. Zeller, and P.H. Dederichs, *ibid.* **54**, 14 121 (1996); K. Wildberger, P.H. Dederichs, P. Lang, V.S. Stepanyuk, and R. Zeller (unpublished).
- ²¹S. Blügel, B. Drittler, R. Zeller, and P.H. Dederichs, Appl. Phys. A **49**, 547 (1989).
- ²²F. Liu, M.R. Press, S.N. Khanna, and P. Jena, Phys. Rev. B **39**, 6914 (1989).
- ²³T.G. Walker and H. Hopster, Phys. Rev. B **48**, 3563 (1993).
- ²⁴S. Andrieu, M. Finazzi, F. Yulero, H.M. Fischer, Ph. Arcade, F. Chevrier, L. Hennes, K. Hricovini, G. Krill, and M. Piecuch, Europhys. Lett. **38**, 459 (1997).
- ²⁵O. Rader, W. Gudat, D. Schmitz, C. Carbone, and W. Eberhardt, Phys. Rev. B **56**, 5053 (1997); J. Dresslhaus, D. Spanke, F.U. Hillebrecht, E. Kisker, G. van der Lann, J.B. Goedkoop, and N.B. Brookes, *ibid.* **56**, 5461 (1997).
- ²⁶V.S. Stepanyuk, W. Hergert, P. Rennert, K. Wildberger, R. Zeller, and P.H. Dederichs, Solid State Commun. **101**, 559 (1997); V.S. Stepanyuk, W. Hergert, K. Wildberger, S.K. Nayk, and P. Jena, Surf. Sci. Lett. **384**, L892 (1997).
- ²⁷R. Sessoli, D. Gatteschl, A. Caneschl, and M.A. Novak, Nature (London) **365**, 141 (1993).
- ²⁸L. Zhong and A.J. Freeman, J. Appl. Phys. **81**, 3890 (1997).
- ²⁹Our calculations show that the magnetic moment of Ru atom in the *H* position on unsupported fcc Fe monolayer is $1.4\mu_B$, i.e., the Cu substrate strongly reduces magnetic moments (see Fig. 4).